Research Square

Preprints are preliminary reports that have not undergone peer review.
They should not be considered conclusive, used to inform clinical practice,
or referenced by the media as validated information.

Distribution fractions and potential ecological risk assessment of heavy metals in mangrove sediments of the Greater Bay Area

Huan-Zhan Zhou
Jinan University
Jun-Feng Wang
Jinan University
Hui-Min Jiang
Jinan University
Ze-Xiang Cai
Jinan University
Guan-Hui Tang
Jinan University
Ding Song
Jinan University
Sheng-Teng Liu
Jinan University
ZhiMin Xu (xuzhimin@zhku.edu.cn)
Zhongkai University of Agriculture and Engineering

Research Article

Keywords: Mangrove restoration, Heavy metals, Ecological risk assessment, Coastal Sediment, Redundancy Analysis

Posted Date: September 27th, 2022

DOI: https://doi.org/10.21203/rs.3.rs-2011793/v1

License: This work is licensed under a Creative Commons Attribution 4.0 International License. Read Full License

Version of Record: A version of this preprint was published at Environmental Science and Pollution Research on January 28th, 2023. See the published version at https://doi.org/10.1007/s11356-023-25551-2.

Abstract

The restoration of mangrove forests in coastal wetlands of China were constantly established since 1990s. However, various pollutants, especially for heavy metals (HMs), discharged with wastewater might present a significant risk to mangrove forests during the restoration. In this study, sediments of five typical mangrove wetlands with varying restoration years and management measures were collected to evaluate the distribution fractions and potential ecological risk of HMs in the Greater Bay Area (GBA). Cd (0.2–1.6 mg/kg) was found in high concentrations in the exchangeable fraction (37.8–71.5%), whereas Cu (54.2–94.8 mg/kg), Zn (157.6-332.6 mg/kg), Cr (57.7-113.6 mg/kg), Pb (36.5–89.9 mg/kg) and Ni (29.7–69.5 mg/kg) primarily presented in residual fraction (30.8–91.9%). According to the geo-accumulation index (I_{geo}) analysis, sediment Cd presented high level of pollution ($3 \leq I_{geo} \leq 4$), while Zn and Cu showed with moderately pollution ($1 \leq I_{geo} \leq 2$). Besides, high ecological risk of Cd was found in sediments of five mangroves, with risk assessment code (RAC) ranging from 45.9 to 84.2. Redundancy analysis revealed that the content of NO_3^--N was closely related to that of HMs in sediments and, pH value and NO_3^--N concentration affected the distribution of HMs geochemical fractions. Furthermore, pollutants discharged from industrial activities rather than mangrove forest planting years determined the pollution levels of HMs. Fortunately, strict drainage standards for industrial activities in Shenzhen significantly availed for decreasing HMs contents in mangrove sediments. Therefore, future development of mangrove conversion and restoration should be linked to the water purification in the GBA.

1. Introduction

Despite occupying no more than 0.06% of the earth's surface, mangrove ecosystem actually played an important role in water purification, wind/waves protection and carbon restoration (De Lacerda & Linneweber, 2002; FIELD et al., 1998; Hamilton & Casey, 2016). Due to anthropogenic activities' negative effects, e.g., urbanization and aquaculture, coastal areas for mangrove forests growth have been significantly decreased by ~ 40% worldwide over the past half-century (Herbeck et al., 2020). Fortunately, with the increase of environmental protection awareness and the development of social economy of developing countries, especially for China, the conservation and restoration of mangrove forests in coastal wetlands were rapidly established since 1990s (Herbeck et al., 2020). However, the continuous discharge of pollutants from anthropogenic activities accomplished by industrial development might be still a seriously potential threat to mangrove forests, especially for that in restoration processes (Lewis et al., 2011; Maiti & Chowdhury, 2013). Recently, scarce information is presented concerning the potential ecological threats of anthropogenic pollutants on mangrove forests with varying restoration years.

As representative pollutants, heavy metals (HMs), mainly discharging from industrial activities into estuary areas (Algül & Beyhan, 2020), presented a significant risk to mangrove ecosystem (Feng et al., 2017; Tam & Wong, 2000; Zhang et al., 2014). The particularity of mangrove ecosystem was benefit for fine sediments, organics and minerals deposition, indirectly promoting the accumulation of HMs in the relevant sediments (Prasad & Ramanathan, 2008; Shao et al., 2009). In addition, the geochemical fractions of HMs in sediments might be transformed with acid dissolution and complexation effects (Kostka & Luther III, 1994; Zhang et al., 2017). It is generally agreed that bioavailable HMs in sediments could be easily accumulated by mangrove forests, resulting in a serious risk to plant health. This was mainly attributed to two reasons: (i) anions, e.g., Cl^-, SO_4^{2-}, migrated with tidal process could complex with HMs (Hirsch et al., 1989; Weggler et al., 2004); (ii) protons, organic acids and amino acids secreted by microorganisms and mangroves availed for soil acidification and lead to the increase amount of HMs in bioavailable HMs fractions (Wang et al., 2021). Furthermore, mangrove forests also played a significant part in the uptake of HMs from sediments, but this effect was significantly different due to the differences of mangrove growth stages (Feng et al., 2017). However, there is still a lack of relevant information on the relationships between HMs distribution characteristics and external pollutants or physicochemical properties of mangrove sediments in restoration stages.

The Greater Bay Aera (GBA), located in (sub)tropical regions, including Hong Kong, Macao and nine cities in Guangdong. There are obvious differences in industrial distribution and economic level due to varying development emphasis among these cities. Comparatively, cities on the East Bank of the GBA presented with more electronic manufacturing factories than that on the West Bank, resulting in certain differences in pollutant discharge amount during the industrial activities. In addition, there are certain differences in the treatment standards of industrial wastes among these cities with varying urban environmental policies (Yang

et al., 2012), resulting in the different fractions and concentrations of HMs discharged into surrounding mangrove ecosystem. In addition, planting years of mangroves in various regions significantly varied due to the differences in restoration time, which might affect the tolerance of mangroves to HMs pollutants (Bai et al., 2011). Therefore, it is of great significance to understand the differences of human activities and urban development on the HMs distribution features of mangrove wetlands in the GBA.

Therefore, five representative mangroves sites with certain differences in planting years and industrial activities were selected for sediments sampling in the GBA. The study's objectives were: (i) to determine the relationship between sediment HMs concentration and urban effluent nutrients (e.g., AP, NH_4^+, NO_3^-); (ii) to estimate the influences of varying physiochemical properties on the geochemical fractions of HMs in sediments; (iii) to evaluate the effects of industrial development and environmental protection on HMs accumulation in mangrove sediments.

2. Materials And Methods

2.1. Study area

The GBA is located in southern China, with an annual mean temperature of 21.4–22.4°C and an annual average precipitation of 1662.7 mm (2020). As one of the most economically developed regions in China, extensive industrial and anthropogenic activities in this area have caused a relatively serious HM contamination (Zhang et al., 2017). It has been confirmed many surface water in this area contained with trace metals from mining, industrial, and agricultural activities (Zhao et al., 2017). According to the annual detection data of National Estuary in 2021, the main pollutants in aquatic environment were nitrogen and HMs. For instance, total nitrogen concentrations in river sections of Guangzhou (GZ), Shenzhen (SZ), Zhuhai (ZH) and Jiangmen (JM) were 2.2, 0.8, 0.6 and 0.5 mg/L, respectively.

Coastal ecosystems, especially for mangrove wetland system, with outstanding HM and nutrient retention capacity take a significant part in the environmental protection of terrestrial-marine transitions. Therefore, to reveal the influence factors, e.g., human activity, regional protection policies and restoration age, on the ecological function of mangrove wetlands, five mangrove wetland sites were selected within the GBA at wet season of 2021. Two sampling points with three replicates of each mangrove wetland in Beidou (BD), Qi'ao Island (QA), Nansha (NS), Hai'ou Island (HO), and Futian (FT) (Fig. 1), which are located in JM, ZH, GZ, GZ, SZ, respectively. NS site exhibits with natural mangrove forest (at least 40 years), while the mangrove restoration ages of mangrove forest at BD, QA, HO, and FT sites are approximately 10, 20, 5, and 3 years, respectively. Given that population density and protective measure of local situation, mangroves in BD, QA and FT sites as affected by human activity are relatively weaker than that in NS and HO sites. The invasion of alien species, e.g., *Spartina alterniflora, Mikania micrantha Kunth*, and *Leucaena leucocephala*, in QA site occurred 18–24 years ago. While FT site was introduced with *Aegiceras corniculatum*, *Kandelia obovataa sheue* and *Avicennia marina* 3 years ago, after the remove of alien species *Sonneratia apetala*, which has been planted for 17 years.

2.2. Sediment sampling and chemical analyses

Mangrove surface sediments at two depths of 0–20 and 20–40 cm from BD, QA, NS, HO, and FT sites were collected in the GBA (Fig. 1). After collection, they were immediately stored in car refrigerators and then prepared for subsequent analyses in the laboratory. After two weeks of air drying at room temperature, all samples were screened through a 2 mm sieve to remove small gravel and coarse debris. Each dried sample was ground until every particle passed through a 0.149 mm nylon sieve for determination of physicochemical properties and HMs fractions.

Sediment pH was determined using a calibrated pH meter (HQ40D, Hach, USA) with the supernatant collected from soil-water mixture liquid at a soil-water weight ratio of 1:5. Sediment organic carbon (SOC) was analyzed with an elemental analyzer (vario TOC Cube, Elementar, Germany). The concentrations of nitrogen (NH_4^+-N and NO_3^--N forms) and available phosphorus in sediments were detected according to the standards of HJ 634–2012 and NY/T 1121.7–2014, respectively. The total HMs, e.g., Cu, Zn, Cd, Cr, Pb, Ni, were determined by ICP-MS (NexION 350, Shimadzu, Japan) after digestion with hydrochloric acid and nitric acid in the ratio of 1:3. According to a five-step process suggested by Tessier et al. (1979) (Tessier et al., 1979), sediment HMs were extracted and classified into five fractions, including exchangeable fraction (F1), carbonate fraction (F2), Fe-Mn oxide

fraction (F3), organically bound fraction (F4), and residual fraction (F5), respectively. For HMs concentration tests, blank and standard reference materials (GBW07401) were injected into ICP-MS for evaluating the determination process's accuracy and precision. The recovery rate of samples spiked with internal and recovery standards maintained at the ranges of 95% and 105%.

2.3. Geo-accumulation index (I_{geo})

The geographic accumulation index (I_{geo}) was used to evaluate the contamination situation of HMs in mangrove sediments, which is defined by Eq. (1) (Muller, 1969) as

$$I_{geo}=\log_2 \frac{C_n}{1.5\times B_n} \quad (1)$$

where C_n and B_n represent the measured concentration of HM n in the sediment and the geological background value of HM n, respectively. The constant term 1.5 takes the consideration of the fluctuation of HMs background value in sediments caused by possible lithological variations (Ma et al., 2016). Zn, Cr, Cu, Ni, Cd, and Pb in the GBA have background concentrations of 47.3, 50.5, 17, 18.2, 0.056, and 36 mg/kg, respectively (Chen et al., 1991). According to I_{geo} values, the pollution situation of each HM is divided into seven levels: $I_{geo}\leq 0$: unpolluted, $0 < I_{geo}\leq 1$: weakly polluted, $1 < I_{geo}\leq 2$: moderately polluted, $2 < I_{geo}\leq 3$: moderately to heavily polluted, $3 < I_{geo}\leq 4$: heavily polluted, $4 < I_{geo}\leq 5$: heavily to and extremely polluted; $I_{geo}>5$: extremely polluted.

2.4. Risk assessment code (RAC)

The mobility and bioavailability of HM n is assessed by the RAC according to its proportion of exchangeable and carbonate fractions to the total fractions in sediments, which is defined by Eq. (2) as

$$RAC_i=\frac{Metal_{ef}^i+Metal_{cf}^i}{Metal_t^i}\times 100 \quad (2)$$

where $Metel_{ef}$, $Metel_{cf}$, and $Metel_t$ represent the concentration of HM n in exchangeable fraction, carbonate fraction, and the sum of all fractions, respectively. According to assessment results, the RAC indices are divided into five levels: RAC ≤ 1: no risk (NR), 1 < RAC ≤ 10: low risk, 10 < RAC ≤ 30: medium risk, 30 < RAC ≤ 50: high risk, and 50 < RAC ≤ 100: very high risk (Marrugo-Negrete et al., 2017).

2.5. Statistical analysis

The differences of physicochemical properties and HM concentration among different mangroves sediments (SPSS 20.0, IBM, USA) were identified by the One-way analysis of variance (ANOVA) and $p < 0.05$ was considered as the significant level. Pearson's correlation test was used to assess the correlation analysis between HMs content and sediment physicochemical properties. Furthermore, redundancy analysis (RDA) was used with canoco 5 for windows to evaluate the relationships between HMs and sediment physicochemical properties.

3. Results

3.1. Physicochemical properties of mangrove sediments

The physicochemical properties of mangrove sediments for surface (0–20 cm) and bottom (20–40 cm) layers in the GBA are presented with Table 1. Five sites of mangrove sediments showed almost no statistically significant difference in pH between two layers ($p > 0.05$); higher pH values were found at the BD and NS sites. The SOC concentration increased with planting years, especially for mangroves that planted over 20 years. With the increase of planting years, the SOC content significantly increased with depth in QA site ($p < 0.05$). The content of NH_4^+-N in sediments of two layers for five sites were substantially higher than that of NO_3^--N. In addition, NH_4^+-N contents in sediments of two layers for five sites showed no obvious pattern, however, NO_3^--

N concentrations in the surface layer (0–20 cm) of five sites were higher than that of bottom layer (20–40 cm). The content of available P in mangrove sediments was significantly higher at the FT site than at the other sampling sites ($p < 0.05$), but there was no statistically significant difference in available P between two layers among five mangrove sediment sites ($p > 0.05$).

Table 1
Physicochemical properties of mangrove sediments (two layers: 0–20 and 20–40 cm) collected from five sampling sites in the GBA (Data: average value ± standard deviation).

Site types	Mangrove age (years)	Sediment layer (cm)	pH	SOC (g/kg)	NH_4^+-N (mg/kg)	NO_3^--N (mg/kg)	Available P (mg/kg)
Site BD (n = 6)	10	0–20	7.3 ± 0.2^{A1}	23.5 ± 3.6^{A1}	20.1 ± 2.7^{A1}	2.6 ± 0.3^{A1}	6.5 ± 0.5^{A1}
		20–40	7.3 ± 0.2^{A1}	22.6 ± 1.6^{A1}	13.8 ± 1.9^{B1}	1.9 ± 0.2^{B1}	6.6 ± 1.2^{A1}
Site QA (n = 6)	20	0–20	6.7 ± 0.2^{A2}	33.3 ± 2.2^{A2}	14.6 ± 2.0^{A2}	3.0 ± 0.3^{A12}	10.3 ± 1.2^{A2}
		20–40	7.0 ± 0.5^{A1}	30.4 ± 1.3^{A2}	12.0 ± 1.3^{B1}	0.7 ± 0.3^{B2}	9.0 ± 3.4^{A2}
Site NS (n = 6)	> 40	0–20	7.1 ± 0.5^{A12}	24.0 ± 1.7^{A1}	9.1 ± 1.2^{A3}	3.3 ± 0.6^{A2}	8.6 ± 0.4^{A12}
		20–40	7.7 ± 0.4^{B2}	18.1 ± 2.2^{B3}	14.7 ± 3.1^{B12}	2.8 ± 0.6^{A3}	5.7 ± 0.5^{B1}
Site HO (n = 6)	5	0–20	6.6 ± 0.4^{A2}	21.0 ± 3.8^{A1}	11.9 ± 1.3^{A23}	4.3 ± 1.0^{A3}	13.2 ± 3.0^{A3}
		20–40	6.8 ± 0.2^{A1}	18.2 ± 2.2^{B3}	16.7 ± 2.4^{B2}	2.8 ± 0.1^{B3}	11.2 ± 1.9^{A3}
Site FT (n = 6)	3^c	0–20	6.9 ± 0.4^{A12}	20.5 ± 1.1^{A1}	7.5 ± 0.3^{A3}	1.1 ± 0.5^{A4}	22.9 ± 3.6^{A4}
		20–40	7.1 ± 0.9^{A1}	21.1 ± 1.3^{A13}	10.6 ± 4.6^{B3}	1.2 ± 0.3^{A4}	28.2 ± 1.6^{B4}

Notes: a. ^{AB} Values in each column with the same letters are not significantly different (LSD) among different sediment layers in same sediment type ($p < 0.05$). b. ^{123} Values in each column with different numbers represent significant differences (LSD) among different mangrove sediment types in same sediment layer ($p < 0.05$). c. Mangrove forests have been planted again for about three years due to the elimination of alien invasion species.

3.2. Total concentrations of heavy metals in mangrove sediments

The average concentrations of HMs in sediments of two layers for five sites ranged from 0.2-369.7 mg/kg and demonstrated the following pattern: Zn > Cr > Cu ≈ Pb > Ni > Cd (Table 2). Generally, the mean values of HMs in two layers of sediments collected from BD and FT sites were lower than that of QA, NS, and HO sites in most cases. In BD site, the contents of Cu, Cd, Cr, and Ni in surface layer (0–20 cm) of sediments were similar with that of bottom layer (20–40 cm) ($p > 0.05$), and the concentration of Zn and Pb in surface layer (0–20 cm) of sediments was significantly lower and higher than that of bottom layer (20–40 cm), respectively ($p < 0.05$). There was no significant difference in HMs content in two layers of sediments from QA site except Cr. In addition, much more Zn, Cr and Pb in surface layer (0–20 cm) of NS site and Cd, Pb, Ni in surface layer (0–20 cm) of HO site were found compared with that of corresponding bottom layer (20–40 cm) ($p < 0.05$). The concentrations of Zn, Cr, and Pb in the surface layer (0–20 cm) of the FT site were significantly lower than those in the bottom layer (20–40 cm) ($p < 0.05$).

Table 2
Total concentrations of HMs, including Cu, Zn, Cd, Cr, Pb, and Ni, in mangrove sediments (two layers: 0–20 and 20–40 cm) collected from five sampling sites in the GBA

Site types	Mangrove age (years)	Sediment layer (cm)	Cu (mg/kg)	Zn (mg/kg)	Cd (mg/kg)	Cr (mg/kg)	Pb (mg/kg)	Ni (mg/kg)
Site BD (n = 6)	10	0–20	54.2 ± 2.5^{A1}	241.7 ± 15.3^{A1}	0.2 ± 0.02^{A1}	72.4 ± 14.9^{A1}	74.2 ± 2.7^{A1}	40.4 ± 9.3^{A1}
		20–40	64.3 ± 4.4^{B1}	260.3 ± 8.9^{B1}	0.3 ± 0.04^{A1}	75.3 ± 8.4^{A1}	48.9 ± 2.4^{B1}	45.5 ± 7.5^{A1}
Site QA (n = 6)	20	0–20	77.8 ± 4.8^{A2}	332.6 ± 14.2^{A2}	0.6 ± 0.04^{A2}	83.8 ± 4.2^{A2}	50.4 ± 3.2^{A2}	45.4 ± 1.4^{A1}
		20–40	84.4 ± 3.0^{A2}	317.2 ± 11.0^{A2}	0.6 ± 0.04^{A2}	93.2 ± 4.1^{B2}	51.4 ± 3.7^{A1}	50.2 ± 3.4^{A1}
Site NS (n = 6)	> 40	0–20	55.7 ± 5.3^{A1}	328.4 ± 13.0^{A2}	0.7 ± 0.06^{A2}	70.8 ± 2.8^{A1}	52.9 ± 1.4^{A2}	38.7 ± 2.3^{A13}
		20–40	89.0 ± 1.3^{B23}	286.8 ± 14.0^{B12}	1.1 ± 0.07^{B3}	64.4 ± 4.1^{B3}	36.5 ± 1.9^{B2}	53.6 ± 15.0^{B1}
Site HO (n = 6)	5	0–20	92.1 ± 4.4^{A3}	306.2 ± 19.2^{A2}	1.6 ± 0.02^{A3}	113.1 ± 25.4^{A3}	89.9 ± 5.9^{A3}	69.5 ± 4.2^{A2}
		20–40	94.8 ± 6.3^{A3}	283.2 ± 17.1^{B12}	1.0 ± 0.18^{B3}	113.6 ± 17.8^{A4}	72.8 ± 5.3^{B3}	59.5 ± 13.4^{B2}
Site FT (n = 6)	3^{c}	0–20	79.7 ± 10.0^{A23}	157.6 ± 9.3^{A3}	0.4 ± 0.03^{A1}	57.7 ± 4.1^{A4}	51.5 ± 6.6^{A2}	29.7 ± 5.8^{A3}
		20–40	71.1 ± 4.8^{B12}	273.1 ± 18.0^{B1}	0.3 ± 0.05^{A1}	75.3 ± 8.3^{B1}	61.2 ± 1.2^{B4}	32.3 ± 2.2^{A3}

Notes: a. ^{AB} Values in each column with the same letters are not significantly different (LSD) among different sediment layers in same sediment type ($p < 0.05$). b. ^{123} Values in each column with different numbers represent significant differences (LSD) among different mangrove sediment types in same sediment layer ($p < 0.05$). c. Mangrove forests have been planted again for about three years due to the elimination of alien invasion species.

3.3. Heavy metals fractions in mangrove sediments

The mean percentage of five geochemical fractions for six HMs in two layers of sediments collected from five mangrove sites in the GBA are illustrated in Fig. 2. Although some minor differences in five extraction fractions were found among these sediment samples, the distribution of HMs fractions exhibited with similar patterns at two sediment layers.

As shown in Fig. 2, the exchangeable fraction of Cd presented with the largest percentage (mean value: 38.6% in BD, 70.4% in QA, 57.1% in NS, 63.6% in HO, and 72.3% in FT) among five sequentially extraction phases. Furthermore, the percentage of residual fraction of Cd in BD and FT sites, and the carbonate fraction of Cd in QA, NS, and HO sites also had a relatively high proportion in surface sediments. The ratio of exchangeable Cd showed a decreasing trend, whereas an opposite tendency was observed for the percentage of carbonate and residual Cd with the increasing depth of sediments. Generally, much higher percentage of exchangeable Cd was observed in mangrove sediments when compared with that of other HMs ($p < 0.05$).

Cr, Pb, Zn and Ni fractions in two sediment layers followed the order: residual > Fe-Mn oxide > organic bound > carbonate bound > exchangeable. The ratios of residual (organic bound) Cr, Pb, Zn and Ni ranged from 46.9%-62.1% and 33.2%-66.5%, respectively. For Fe-Mn oxide fraction, they varied in ranges of 24.2%-37.2% and 26.5%-54.7%, respectively. For sediment Cu, it appeared mostly in residual form in BD and NS, accounting for 89.6 and 69.2% of total amount, respectively. However, Cu in QA,

HO and FT was primarily in the organic bound and residual state, the former and latter fractions accounted for 34.2–41.3% and 42.8–54.6%, respectively.

3.4. Heavy metals pollution and ecological risk assessment

The I_{geo} evaluation for six HMs in two sediment layers of five mangrove sites in the GBA are illustrated in Fig. 3. With the exception of Ni pollution, there was no discernible difference in I_{geo} values between the surface layer (0–20 cm) and the bottom layer (20–40 cm) ($p > 0.05$). The pollution levels of these metals demonstrated the following pattern: Cd > Zn > Cu > Ni > Pb > Cr, I_{geo} values among five sites were as followed: HO > NS > QA > FT > BD. In general, Cd in most sediments among five sites were classified into “heavily polluted” ($3 < I_{geo} \leq 4$). Comparatively, Zn and Cu in these sites showed “moderately polluted” ($1 < I_{geo} \leq 2$) according to I_{geo} analysis. The other metals, including Cr, Pb and Ni, were found with negative I_{geo} values among five sediment sites, indicating an “unpolluted” or “weakly polluted” level.

According to RAC analysis, Cd in mangrove sediments also presented with a high ecological risk, ranging from 45.9 to 84.2 (Fig. 4). The trendies of layer risk and pollution level of these metals in sampling sites were similar with that of I_{geo} evaluation. Notably, RAC value of Cr in five mangrove sediments were showed a low risk (2.3–5.6), while the RAC values of other metals, including Pb, Cu, Zn and Ni, ranged from (0.3-23.51), suggesting a “medium risk” or “low risk” level.

3.5. Relationships between heavy metals and sediment physicochemical properties

The RDA of HMs (Zn, Cr, Cu, Ni, Cd and Pb) and physicochemical properties (pH, SOC, NH_4^+-N, NO_3^--N and available P) among five mangrove sediments were presented with Fig. 5. In general, over 75% of changes in total content of six HMs can be explained by sediment physicochemical properties. The total concentrations of HMs distributed in five mangrove sediments were strongly affected by NO_3^--N and NH_4^+-N. According to RDA ordination diagram, sediments sampled from five mangroves sites exhibited a certain level similarity, especially for that of BD and FT. The Pearson correlation analysis also revealed a significant correlation between the concentrations of HMs and sediment nitrogen, especially for NO_3^--N ($p < 0.05$) (Table 3). In addition, the total concentrations of most HMs in these sediments showed a significant correlation with each other.

Table 3
Spearman correlation analysis among total contents of HMs and physicochemical properties of mangrove sediments in the GBA (n = 60).

	pH	NH_4^+-N	NO_3^--N	SOC	Available P	Cu	Zn	Cd	Cr	Pb	Ni
pH	1.000										
NH_4^+-N	0.135	1.000									
NO_3^--N	-0.227	0.222	1.000								
SOC	-0.257	0.010	-0.155	1.000							
Available P	-0.302	**-0.478****	-0.377	-0.218	1.000						
Cu	-0.266	-0.051	0.116	-0.225	0.110	1.000					
Zn	-0.104	**0.150***	**0.441***	-0.040	-0.394	0.151	1.000				
Cd	-0.241	0.017	**0.678****	-0.267	-0.252	**0.655****	**0.437***	1.000			
Cr	**-0.502****	0.207	**0.371***	-0.350	-0.105	**0.551****	**0.506****	**0.594****	1.000		
Pb	**-0.533****	0.206	**0.439***	-0.237	0.143	0.163	0.076	**0.372***	**0.677****	1.000	
Ni	-0.230	0.155	**0.367***	-0.222	-0.277	**0.466****	0.299	**0.625****	**0.547****	0.325	1.000

Note: a. * Significant correlation at $p < 0.05$; ** Significant correlation at $p < 0.01$. b. The marks in bond represent a significant correlation between two factors in mangrove sediments ($p < 0.05$).

Physicochemical properties of mangrove sediments could also be used to assess the variations of geochemical fractions of HMs (Fig. 6). In general, NO_3^--N was closely related to Fe-Mn bound fraction of six metals except for Cu, and the linear regression correlation of NO_3^--N and Fe-Mn bound state in Table 4 re-confirmed former result. Notably, the linear relationship was more obvious at QA, NS and HO sites with relatively serious HM pollution level. Furthermore, RDA results indicated that the distribution of exchangeable Cd in mangrove sediments was similar with that in carbonate fraction, resulting higher RAC values in the GBA.

Table 4

The linear regression of HMs in Fe-Mn oxide fraction against to NO_3^--N in mangrove sediments of BD, QA, NS, HO and FT in the GBA.

Site types	Metal-types	Regression equation	Adj R^2	F value
BD	Cu-F3	Y=-2.7497X + 7.4618	0.0469	1.6895
	Zn-F3	Y=-7.5754X + 34.6767	0.1220	2.9457
	Cd-F3	Y = 0.0073X + 0.0108	-0.4864	0.3508
	Cr-F3	Y = 1.3131X + 15.8519	-0.1168	0.0583
	Pb-F3	Y = 38.1183X-57.3740	0.0492	2.2116
	Ni-F3	Y=-1.6035X + 6.9666	-0.0293	0.5705
QA	Cu-F3	**Y=-1.5257X + 7.8364**	**0.6433**	**17.2379****
	Zn-F3	**Y=-5.6569X + 98.0280**	**0.4730**	**9.0797***
	Cd-F3	**Y=-0.0272X + 0.0941**	**0.4231**	**7.6027***
	Cr-F3	Y = 4.1053X + 18.3021	-0.0587	0.2226
	Pb-F3	Y=-2.6740X + 25.4184	-0.0531	0.2944
	Ni-F3	**Y=-1.7393X + 13.0415**	**0.2397**	**5.4153***
NS	Cu-F3	**Y=-1.8076X + 12.7328**	**0.2603**	**6.3862***
	Zn-F3	**Y = 31.5373X-10.3138**	**0.4296**	**11.5448****
	Cd-F3	Y=-0.1368X + 0.5276	-0.0231	0.6830
	Cr-F3	Y = 5.7720X + 2.1230	-0.0749	0.0244
	Pb-F3	Y = 19.0438X-39.4772	-0.0455	0.3897
	Ni-F3	**Y = 5.0341X-4.8843**	**0.2640**	**6.7468***
HO	Cu-F3	**Y=-0.1584X + 8.5162**	**0.3265**	**7.7887***
	Zn-F3	**Y = 1.5640X + 122.9617**	**0.3818**	**9.6496****
	Cd-F3	Y=-0.0157X + 0.2253	0.0482	2.0116
	Cr-F3	Y=-0.9562X + 38.7867	-0.0393	0.4705
	Pb-F3	**Y = 14.9639X-12.7005**	**0.2617**	**6.4669***
	Ni-F3	Y = 2.1598X + 21.6094	-0.0093	0.8699
FT	Cu-F3	**Y=-8.8846X + 18.9624**	**0.7456**	**42.0430*****
	Zn-F3	Y = 78.9006X-33.0277	0.0448	1.6566
	Cd-F3	Y=-0.1273X + 0.1598	-0.0581	0.2306

Note: a. X and Y mean the concentration of NO_3^--N and HMs in Fe-Mn oxide fraction, respectively. b. *, ** and *** present the significant correlation at $p < 0.05$, $p < 0.01$ and $p < 0.001$, respectively. c. The marks in bond represent a significant correlation between the concentrations of NO_3^--N and HMs in Fe-Mn oxide fraction in mangrove sediments ($p < 0.05$).

Site types	Metal-types	Regression equation	Adj R^2	F value
	Cr-F3	Y = 29.1721X-17.5863	-0.0440	0.4099
	Pb-F3	Y = 72.6319X-68.0773	-0.0217	0.7026
	Ni-F3	Y = 26.9721X-25.5607	-0.0462	0.3806

Note: a. X and Y mean the concentration of NO_3^--N and HMs in Fe-Mn oxide fraction, respectively. b. *, ** and *** present the significant correlation at $p < 0.05$, $p < 0.01$ and $p < 0.001$, respectively. c. The marks in bond represent a significant correlation between the concentrations of NO_3^--N and HMs in Fe-Mn oxide fraction in mangrove sediments ($p < 0.05$).

4. Discussions

4.1. Heavy metals fractions in different mangrove sediments

Comparatively, Cd in sediments exhibited relatively higher percentages of exchangeable and carbonate-bound fractions, resulting in more serious ecological risk of Cd in mangrove wetlands. It is generally agreed that soil chloride (Cl) availed for Cd leaching from solid soil and promoted its mobility (Weggler et al., 2004) due to the complexation effect between two ions (Hirsch et al., 1989). In this study, the salinity values of surface water of these sites were 2.3%, 1.3%, 0.2%, 0.6% and 2.0% in BD, QA, NS, HO and FT, respectively, in which the exchangeable Cd proportion at QA, NS, HO, and FT sites was significantly positive correlated with salinity. In addition, Cd had a specific affinity for carbonates and might participate with carbonate minerals under alkaline condition, resulting in a high proportion of carbonated Cd (Ahdy & Youssef, 2011). This study also implied that sediments pH in the GBA presented neutral to weakly alkaline condition (Table. 1), which rationalized a high amount of carbonate-bound Cd.

The distribution of Cr, Ni, and Zn fractions in GBA mangrove sediments was mainly concentrated in residual fraction, derived from natural weathering and their compounds with silicate, leading to a low ecological risk (Ngiam & Lim, 2001; Xiao et al., 2015). Sediments Cu exhibited a larger proportion of organic-bound fraction, which is consistent with previous studies (Esmaeilzadeh et al., 2016). Organic matter in sediments serves as the main ligand for Cu complexation and avails for the formation of organic-bound Cu (Krupadam et al., 2007). However, the change of redox potential in sediments could drive its release, causing an adverse effect to mangrove forest (Wu et al., 2016). Highest proportion of organic-bound Cu was found in HO and FT sites, resulting from the frequently withered leaves with Cu replaced Mg in chlorophyll during the first several years after mangrove planting (Wang et al., 2018). Specifically, Pb showed a higher percentage in Fe-Mn oxide, which can be explained by its coprecipitation with Fe and Mn (Li et al., 2014). What is more, the higher concentrations of Fe and Mn (Fe: 2.4–4.9%, Mn: 278.9-1101.2 mg/kg) in the GBA was benefit for its formation in Fe-Mn oxide.

4.2. Effects of sediment physicochemical properties on heavy metals distribution

It is agreed that environmental conditions should be responsible for the changes in bioavailability and mobility of HMs in sediments, whereas the interactive effects between mangroves and their surrounding environment were more intensive due to the frequent transitions of land-salt water and long immersion period of mangroves in the GBA (Bartoli et al., 2012; Tam & Wong, 1995). In this study, HMs content in sediments was negatively correlated with soil pH value (Fig. 5), indicating that lower pH value availed for the mobilization of HMs (de Souza Machado et al., 2016). RDA results also confirmed that pH showed a negative correlation with exchangeable fractions of HMs, except for Cu and Cr (Fig. 6), while the residual and organic-bound states of Cu, Zn and Cd in sediments presented a positive correlation with sediment pH. This demonstrated that HMs adsorption capacity of sediment gradually weakened with increasing pH value, thus affecting the distribution of HMs geochemical fractions in sediments (Bang & Hesterberg, 2004).

Spearman correlation analysis indicated that sediment nitrogen content was significantly related to HMs, particularly for NO_3^--N concentration (Table 3; $p < 0.05$), which could be brought by the anthropogenic sources of HMs and NO_3^--N (Qiao et al., 2022). In

addition, HMs content in Fe-Mn oxide fractions were strongly correlated with NO_3^--N, especially in QA, NS and HO sites, which supported former hypothesis of this study. Furthermore, the investigations overlying water of surface sediment with higher levels of N and P in aquatic environment contributed to more HMs release into sediment (Fu et al., 2014). Hence, NO_3^--N content presented a significant positive correlation with the majority of exchangeable HMs, except for Cr and Pb, suggesting that NO_3^--N enrichment could increase the ecological risks of Cr and Pb to mangrove systems (Qiao et al., 2022). The reasons may be concluded into: (i) sulfur autotrophic denitrification process availed for the production of SO_4^{2-}, resulting in transformation of HMs from stable oxidizable state to exchangeable fraction (Shao et al., 2009); (ii) the changes of rhizosphere metabolism after nitrogen absorption, inducing the secretion of organic acids and the mobilization of HMs (Wang et al., 2021).

4.3. Human activities and mangrove forest planting years impacted on heavy metals distribution

It is generally agreed that human activities, i.e., sewage discharging and mineral smelting, presented a significant influence on the pollution concentrations and geochemical fractions of HMs (Cai et al., 2007; Ogundiran & Osibanjo, 2009). Due to the huge differences of social economy and industrial activities in the GBA areas, mangroves in GZ and SZ are greatly exposed to external HMs drain pressure than those in ZH and JM (Feng et al., 2017). Comparatively, HMs in mangrove sediments of BD site highly concentrated in residual fraction and remained at moderate pollution levels, indicating that those HMs might be more significantly impacted by geological sources than by industrial activities (Cai et al., 2007; Liang et al., 2022). Notably, a relatively low pollution level was also found in FT, located in SZ region, might be attributable to the implement of water pollution control since 2016, resulting in the surrounding water purification (Huang et al., 2021; Zhou et al., 2021). This confirmed that strict social management strategies could provide the improvement of aquatic environment and decrease the HMs pollution levels in mangrove sediments (Tam & Wong, 2000).

A longer mangrove forest planting years mean that those plants could accumulated more HMs from sediments, resulting in the decrease of HMs in coastal wetlands (Feng et al., 2017). However, results of this study were inconsistent with former reports, which might be caused by: (i) QA, NS and HO sites frequently accompanied by a continuous input of HMs under formerly discharge standards for industrial wastewater; (ii) the re-cultivation of mangrove forests in FT site has been lasted for over 15 years, whereas the plants in sampling site of FT was reclaimed in recent 3 years; (iii) aquatic salinity varied with sampling sites, resulting in a significant impact on the absorption and distribution of sediment HMs (Hirsch et al., 1989). Despite there was no consist character for mangrove forest planting years affecting the HMs distribution, Cd in all sediments exhibited with a high ecological risk value, indicating that the inflow of exogenous Cd exceeded the absorption capacity of mangroves at length (Feng et al., 2017; Li et al., 2007).

5. Conclusions

Sediments of five mangrove wetlands in the GBA were seriously contaminated by Cd and, sediment Cd was highly concentrated in the exchangeable and carbonate-bound fractions. A strong correlation between the concentrations of HMs and NO_3^--N was found in mangrove sediments due to the continuous input of HMs and NO_3^--N with the Pearl River. Further analysis demonstrated that pH value and NO_3^--N concentration affected the distribution of HMs geochemical fractions in sediments. Despite extensive projects have been performed for mangrove restoration, this study found that sediments of mangrove still suffer with relatively serious HMs pollution, especially for Cd. Fortunately, the increase of environmental protection awareness and the development of social economy, strict drainage standards for industrial activities in SZ significantly availed for decreasing HMs contents in mangrove sediments of FT. Therefore, future development of mangrove conversion and restoration should be linked to the water purification management in the GBA.

Declarations

Author contribution

Huan-Zhan Zhou, Hui-Min Jiang & Ze-Xiang Cai: Methodology, Investigation. Jun-Feng Wang: Writing-review & editing, Funding acquisition. Zhi-Min Xu: Review & editing, Project administration, Supervision, Funding acquisition. Guan-Hui Tang, Song Ding & Sheng-Teng Liu: Review & editing.

Founding

This work was supported by the Key Project of National Natural Science Foundation of China (U1901212).

Ethical Approval and Consent to Participate

Not applicable

Consent to Publish

Not applicable

Competing Interests

The authors declare that they have no competing interests

Availability of data and materials

The datasets used and/or analyzed during the current study are available from the corresponding author on reasonable request.

References

1. Ahdy, H.H.H., Youssef, D.H. 2011. Fractionation analysis of some heavy metals in sediments of the north-western part of the Red Sea, Egypt. *Chemistry and Ecology*, **27**(5), 427-443.
2. Algül, F., Beyhan, M. 2020. Concentrations and sources of heavy metals in shallow sediments in Lake Bafa, Turkey. *Scientific reports*, **10**(1), 1-12.
3. Bai, J., Xiao, R., Cui, B., Zhang, K., Wang, Q., Liu, X., Gao, H., Huang, L. 2011. Assessment of heavy metal pollution in wetland soils from the young and old reclaimed regions in the Pearl River Estuary, South China. *Environmental pollution*, **159**(3), 817-824.
4. Bang, J., Hesterberg, D. 2004. Dissolution of trace element contaminants from two coastal plain soils as affected by pH. *Journal of Environmental Quality*, **33**(3), 891-901.
5. Bartoli, G., Papa, S., Sagnella, E., Fioretto, A. 2012. Heavy metal content in sediments along the Calore river: relationships with physical–chemical characteristics. *Journal of Environmental Management*, **95**, S9-S14.
6. Cai, Q.-Y., Mo, C.-H., Wu, Q.-T., Zeng, Q.-Y., Katsoyiannis, A. 2007. Concentration and speciation of heavy metals in six different sewage sludge-composts. *Journal of Hazardous Materials*, **147**(3), 1063-1072.
7. Chen, J., Wei, F., Zheng, C., Wu, Y., Adriano, D.C. 1991. Background concentrations of elements in soils of China. *Water, Air, and Soil Pollution*, **57**(1), 699-712.
8. De Lacerda, L.D., Linneweber, V. 2002. *Mangrove ecosystems: function and management*. Springer Science & Business Media.
9. de Souza Machado, A.A., Spencer, K., Kloas, W., Toffolon, M., Zarfl, C. 2016. Metal fate and effects in estuaries: a review and conceptual model for better understanding of toxicity. *Science of the Total Environment*, **541**, 268-281.
10. Esmaeilzadeh, M., Karbassi, A., Moattar, F. 2016. Assessment of metal pollution in the Anzali Wetland sediments using chemical partitioning method and pollution indices. *Acta Oceanologica Sinica*, **35**(10), 28-36.
11. Feng, J., Zhu, X., Wu, H., Ning, C., Lin, G. 2017. Distribution and ecological risk assessment of heavy metals in surface sediments of a typical restored mangrove–aquaculture wetland in Shenzhen, China. *Marine pollution bulletin*, **124**(2), 1033-

1039.

12. FIELD, C., OSBORN, J., HOFFMAN, L., POLSENBERG, J., ACKERLY, D., BERRY, J., Björkman, O., Held, A., MATSON, P., MOONEY, H. 1998. Mangrove biodiversity and ecosystem function. *Global Ecology & Biogeography Letters*, **7**(1), 3-14.
13. Fu, J., Zhao, C., Luo, Y., Liu, C., Kyzas, G.Z., Luo, Y., Zhao, D., An, S., Zhu, H. 2014. Heavy metals in surface sediments of the Jialu River, China: their relations to environmental factors. *Journal of hazardous materials*, **270**, 102-109.
14. Hamilton, S.E., Casey, D. 2016. Creation of a high spatio-temporal resolution global database of continuous mangrove forest cover for the 21st century (CGMFC-21). *Global Ecology and Biogeography*, **25**(6), 729-738.
15. Herbeck, L.S., Krumme, U., Andersen, T.J., Jennerjahn, T.C. 2020. Decadal trends in mangrove and pond aquaculture cover on Hainan (China) since 1966: mangrove loss, fragmentation and associated biogeochemical changes. *Estuarine, Coastal and Shelf Science*, **233**, 106531.
16. Hirsch, D., Nir, S., Banin, A. 1989. Prediction of cadmium complexation in solution and adsorption to montmorillonite. *Soil Science Society of America Journal*, **53**(3), 716-721.
17. Huang, J., Wang, D., Gong, F., Bai, Y., He, X. 2021. Changes in Nutrient Concentrations in Shenzhen Bay Detected Using Landsat Imagery between 1988 and 2020. *Remote Sensing*, **13**(17), 3469.
18. Kostka, J.E., Luther III, G.W. 1994. Partitioning and speciation of solid phase iron in saltmarsh sediments. *Geochimica et Cosmochimica Acta*, **58**(7), 1701-1710.
19. Krupadam, R.J., Ahuja, R., Wate, S.R. 2007. Heavy metal binding fractions in the sediments of the Godavari estuary, East Coast of India. *Environmental Modeling & Assessment*, **12**(2), 145-155.
20. Lewis, M., Pryor, R., Wilking, L. 2011. Fate and effects of anthropogenic chemicals in mangrove ecosystems: a review. *Environmental pollution*, **159**(10), 2328-2346.
21. Li, J., Pu, L., Zhu, M., Liao, Q., Wang, H., Cai, F. 2014. Spatial pattern of heavy metal concentration in the soil of rapid urbanization area: a case of Ehu Town, Wuxi City, Eastern China. *Environmental Earth Sciences*, **71**(8), 3355-3362.
22. Li, Q., Wu, Z., Chu, B., Zhang, N., Cai, S., Fang, J. 2007. Heavy metals in coastal wetland sediments of the Pearl River Estuary, China. *Environmental Pollution*, **149**(2), 158-164.
23. Liang, F., Pan, Y., Peng, H., Zeng, M., Huang, C. 2022. Time-Space Simulation, Health Risk Warning and Policy Recommendations of Environmental Capacity for Heavy Metals in the Pearl River Basin, China. *International Journal of Environmental Research and Public Health*, **19**(8), 4694.
24. Ma, X., Zuo, H., Tian, M., Zhang, L., Meng, J., Zhou, X., Min, N., Chang, X., Liu, Y. 2016. Assessment of heavy metals contamination in sediments from three adjacent regions of the Yellow River using metal chemical fractions and multivariate analysis techniques. *Chemosphere*, **144**, 264-272.
25. Maiti, S.K., Chowdhury, A. 2013. Effects of anthropogenic pollution on mangrove biodiversity: a review. *Journal of Environmental Protection*, **2013**.
26. Marrugo-Negrete, J., Pinedo-Hernandez, J., Diez, S. 2017. Assessment of heavy metal pollution, spatial distribution and origin in agricultural soils along the Sinu River Basin, Colombia. *Environ Res*, **154**, 380-388.
27. Muller, G. 1969. INDEX OF GEOACCUMULATION IN SEDIMENTS OF THE RHINE RIVER. *GeoJournal*, **2**, 108-118.
28. Ngiam, L.-S., Lim, P.-E. 2001. Speciation patterns of heavy metals in tropical estuarine anoxic and oxidized sediments by different sequential extraction schemes. *Science of The Total Environment*, **275**(1), 53-61.
29. Ogundiran, M., Osibanjo, O. 2009. Mobility and speciation of heavy metals in soils impacted by hazardous waste. *Chemical Speciation & Bioavailability*, **21**(2), 59-69.
30. Prasad, M.B.K., Ramanathan, A. 2008. Sedimentary nutrient dynamics in a tropical estuarine mangrove ecosystem. *Estuarine, Coastal and Shelf Science*, **80**(1), 60-66.
31. Qiao, S., Wang, T., Zhang, Q., Liu, X., Zhao, M. 2022. Distribution Characteristics and Risk Assessment of Heavy Metals in the Source Region of Yangtze River. *Beijing Da Xue Xue Bao*, **58**(2), 297-307.
32. Shao, M., Zhang, T., Fang, H.H. 2009. Autotrophic denitrification and its effect on metal speciation during marine sediment remediation. *Water research*, **43**(12), 2961-2968.

33. Tam, N.F., Wong, Y.S. 1995. Mangrove soils as sinks for wastewater-borne pollutants. *Hydrobiologia*, **295**(1), 231-241.
34. Tam, N.F.Y., Wong, Y.S. 2000. Spatial variation of heavy metals in surface sediments of Hong Kong mangrove swamps. *Environmental Pollution*, **110**(2), 195-205.
35. Tessier, A., Campbell, P.G.C., Bisson, M. 1979. Sequential extraction procedure for the speciation of particulate trace metals. *Analytical Chemistry*, **51**(7), 844-851.
36. Wang, J.-F., Li, W.-L., Li, Q.-S., Wang, L.-L., He, T., Wang, F.-P., Xu, Z.-M. 2021. Nitrogen fertilizer management affects remobilization of the immobilized cadmium in soil and its accumulation in crop tissues. *Environmental Science and Pollution Research*, **28**(24), 31640-31652.
37. Wang, J., Zhu, Q., Shan, Y., Wang, Y., Song, X., Lei, X. 2018. A comparative study on the efficiency of biodegradable EDDS and micro-electric field on the promotion of the phytoextraction by Commelina communis L. in Cu-contaminated soils. *Geoderma*, **314**, 1-7.
38. Weggler, K., McLaughlin, M.J., Graham, R.D. 2004. Effect of chloride in soil solution on the plant availability of biosolid-borne cadmium. *journal of environmental quality*, **33**(2), 496-504.
39. Wu, Q., Zhou, H., Tam, N.F., Tian, Y., Tan, Y., Zhou, S., Li, Q., Chen, Y., Leung, J.Y. 2016. Contamination, toxicity and speciation of heavy metals in an industrialized urban river: implications for the dispersal of heavy metals. *Marine Pollution Bulletin*, **104**(1-2), 153-161.
40. Xiao, R., Bai, J., Lu, Q., Zhao, Q., Gao, Z., Wen, X., Liu, X. 2015. Fractionation, transfer, and ecological risks of heavy metals in riparian and ditch wetlands across a 100-year chronosequence of reclamation in an estuary of China. *Science of The Total Environment*, **517**, 66-75.
41. Yang, Y., Chen, F., Zhang, L., Liu, J., Wu, S., Kang, M. 2012. Comprehensive assessment of heavy metal contamination in sediment of the Pearl River Estuary and adjacent shelf. *Marine Pollution Bulletin*, **64**(9), 1947-1955.
42. Zhang, G., Bai, J., Xiao, R., Zhao, Q., Jia, J., Cui, B., Liu, X. 2017. Heavy metal fractions and ecological risk assessment in sediments from urban, rural and reclamation-affected rivers of the Pearl River Estuary, China. *Chemosphere*, **184**, 278-288.
43. Zhang, Z.-W., Xu, X.-R., Sun, Y.-X., Yu, S., Chen, Y.-S., Peng, J.-X. 2014. Heavy metal and organic contaminants in mangrove ecosystems of China: a review. *Environmental Science and Pollution Research*, **21**(20), 11938-11950.
44. Zhao, G., Ye, S., Yuan, H., Ding, X., Wang, J. 2017. Surface sediment properties and heavy metal pollution assessment in the Pearl River Estuary, China. *Environmental Science and Pollution Research*, **24**(3), 2966-2979.
45. Zhou, Y., Han, J., Li, J., Zhou, Y., Wang, K., Huang, Y. 2021. Building resilient cities with stringent pollution controls: A case study of robust planning of Shenzhen City's urban agriculture system. *Journal of Cleaner Production*, **311**, 127452.

Figures

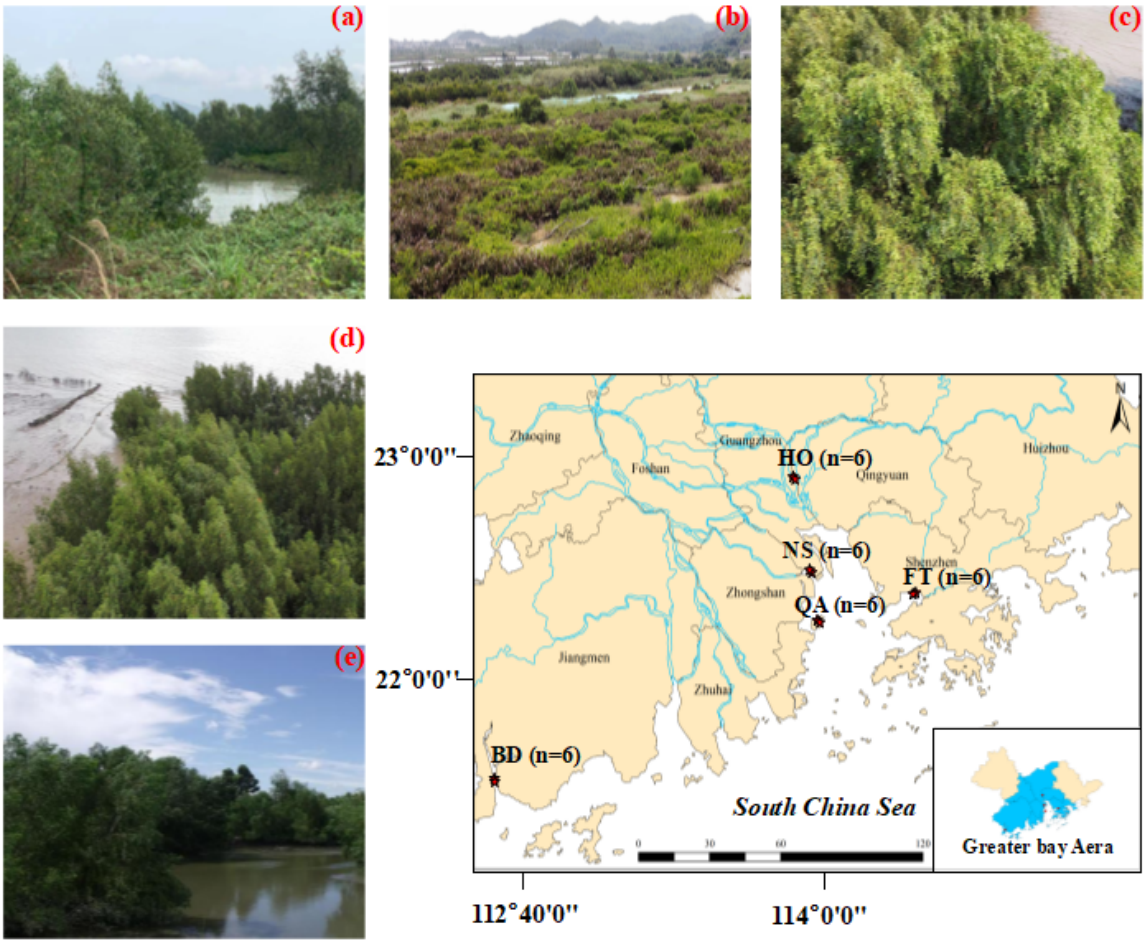

Figure 1

Location map of study area and sampling sites in the GBA. Note: (a), (b), (c), (d) and (e) represent mangrove wetlands in BD, QA, NS, HO and FT sites, respectively.

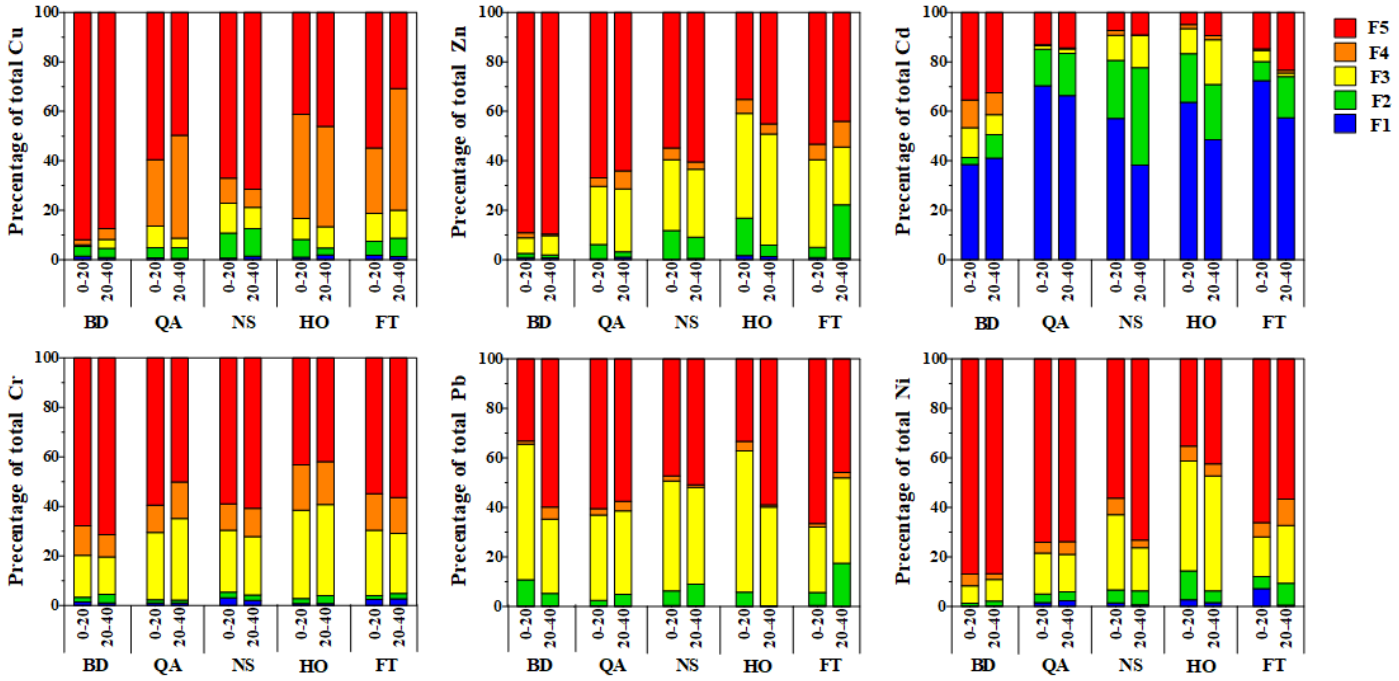

Figure 2

Percentages of five geochemical fractions for Cu, Zn, Cd, Cr, Pb and Ni in two layers (0-20 cm, 20-40 cm) of sediments collected from BD, QA, NS, HO and FT sites, respectively. HMs was classified into exchangeable fraction (F1), carbonate fraction (F2), Fe-Mn oxide fraction (F3), organically bound fraction (F4), and residual fraction (F5), respectively.

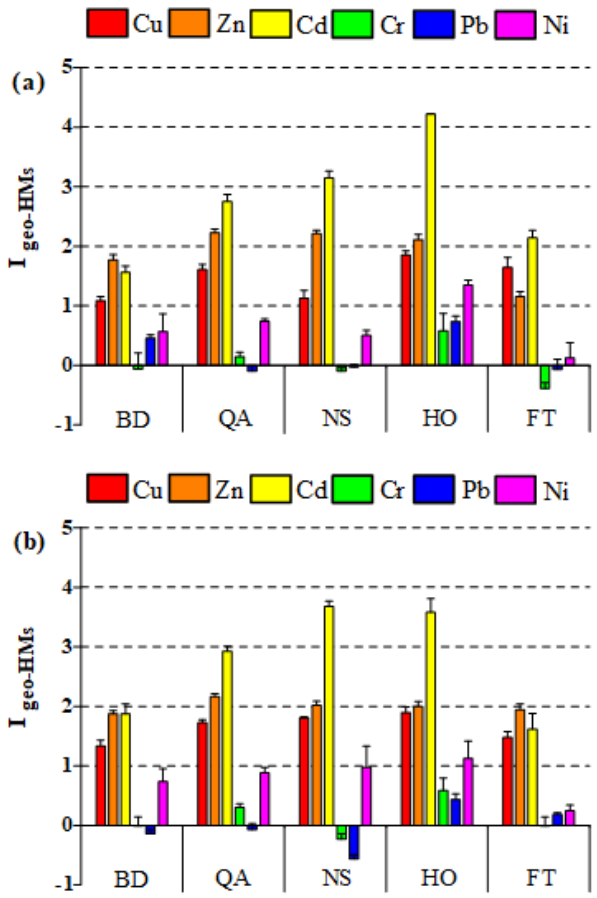

Figure 3

The geo-accumulation index (I_{geo}) of HMs in mangrove sediments (two layers: 0-20 and 20-40 cm) collected from BD, QA, NS, HO and FT sites, respectively. Dotted lines represent different pollution levels.

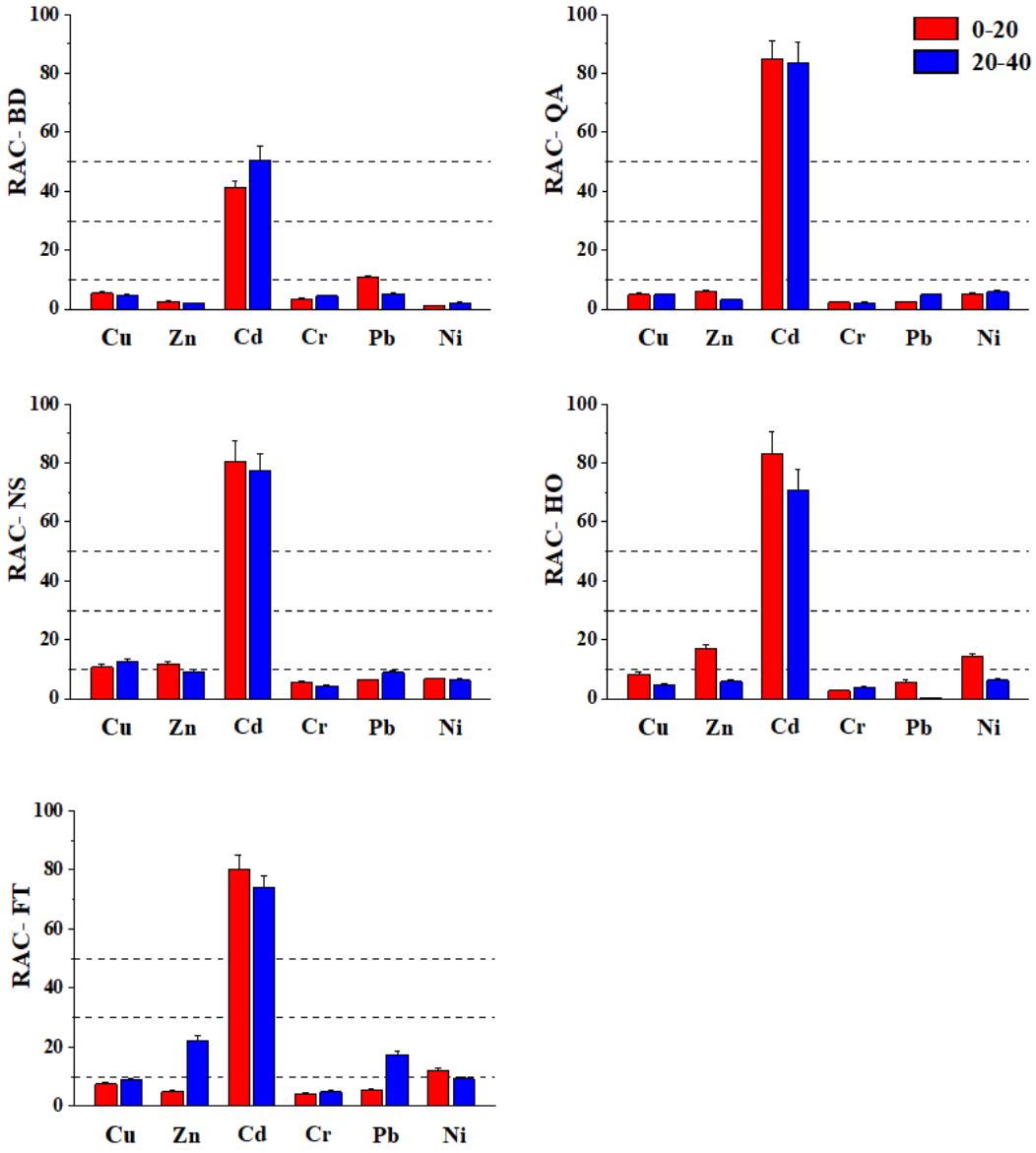

Figure 4

The risk assessment code (RAC) values of Cu, Zn, Cd, Cr, Pb and Ni in mangrove sediments (two layers: 0-20 and 20-40 cm) collected from BD, QA, NS, HO and FT sites, respectively. Dotted lines represent different risk levels.

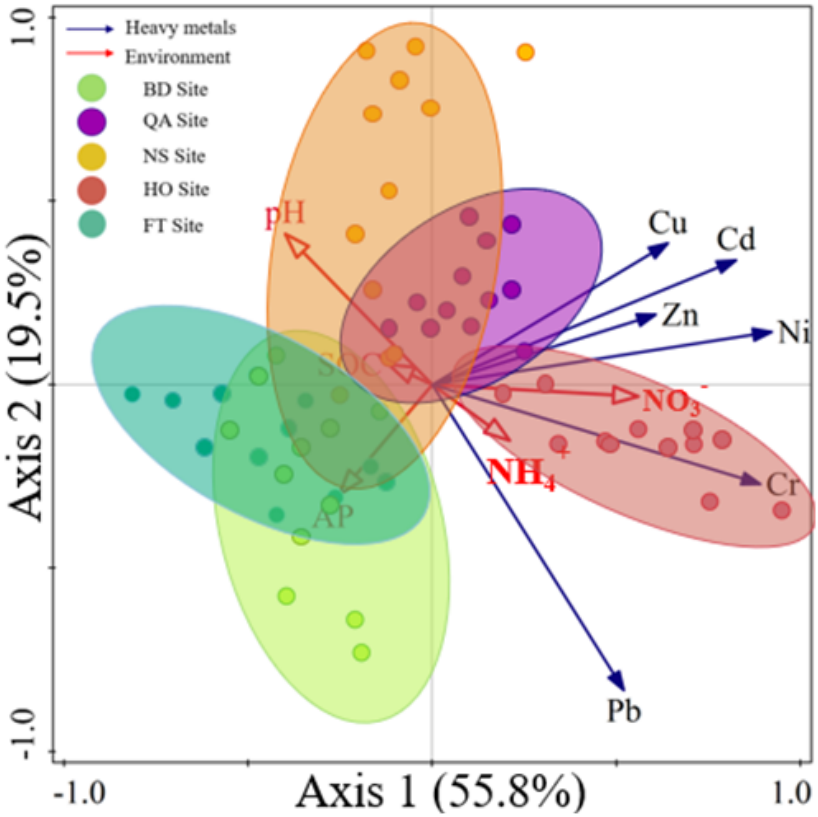

Figure 5

The results of redundancy analysis (RDA) between physicochemical properties and total HMs in mangrove sediments collected from BD, QA, NS, HO and FT sites in the GBA.

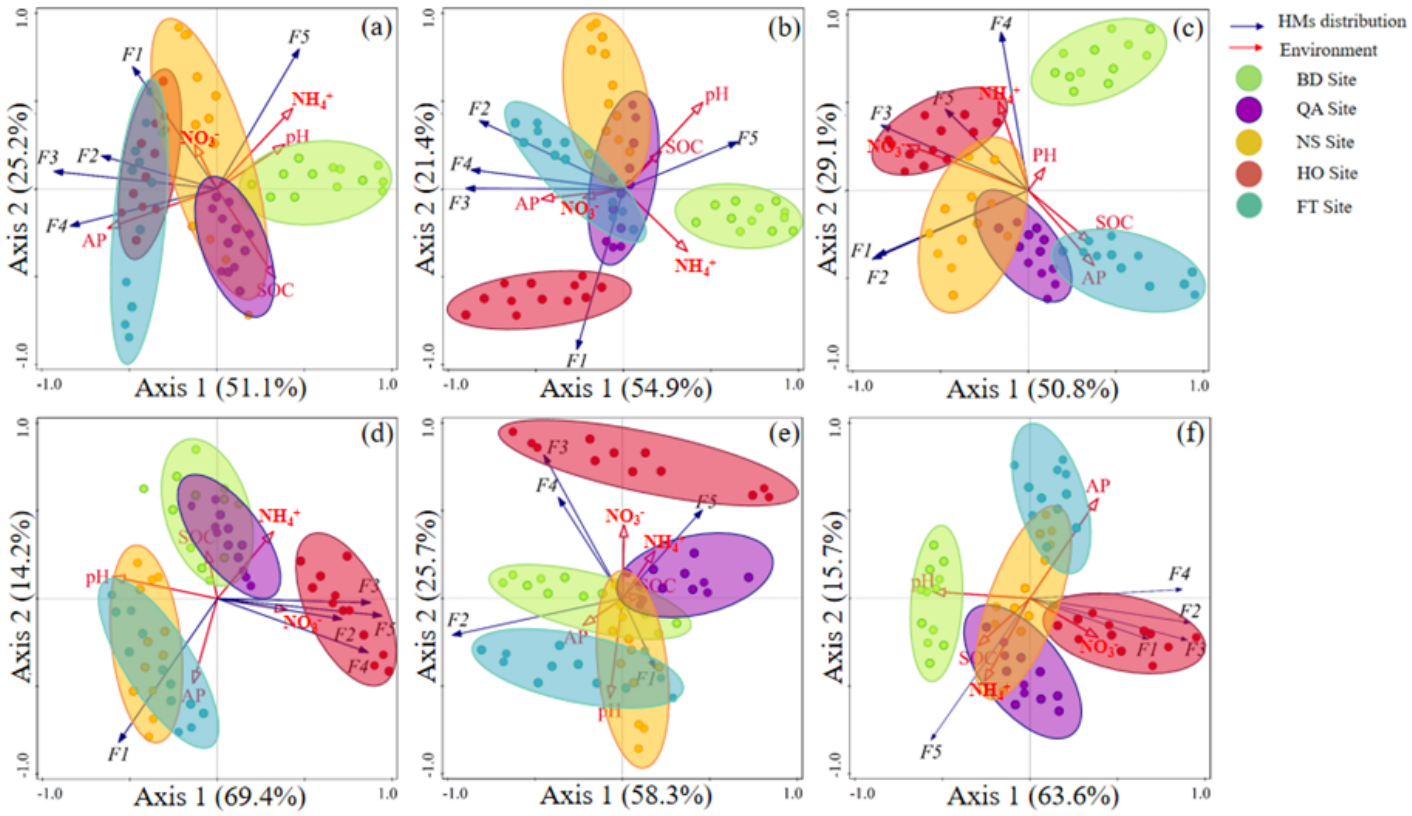

Figure 6

The results of redundancy analysis (RDA) between HMs concentrations in different five geochemical fractions and physicochemical properties in mangrove sediments collected from BD, QA, NS, HO and FT sites in the PRE. (a), (b), (c), (d), (e) and (f) represent Cu, Zn, Cd, Cr, Pb and Ni, respectively.

Supplementary Files

This is a list of supplementary files associated with this preprint. Click to download.

- Supportinginformation202207.docx